

The influence of hydrogen bonds on electron transfer rate in photosynthetic RCs

P.M. Krasilnikov*, P.A. Mamonov, P.P. Knox, V.Z. Paschenko, A.B. Rubin

Biological faculty, M.V. Lomonosov Moscow State University 119899, Moscow, Vorob'evy Gory, Russia

Received 30 September 2006; received in revised form 13 February 2007; accepted 21 February 2007

Available online 15 May 2007

Abstract

Hydrogen bonds formed between photosynthetic reaction centers (RCs) and their cofactors were shown to affect the efficacy of electron transfer. The mechanism of such influence is determined by sensitivity of hydrogen bonds to electron density rearrangements, which alter hydrogen bonds potential energy surface. Quantum chemistry calculations were carried out on a system consisting of a primary quinone Q_A , non-heme Fe^{2+} ion and neighboring residues. The primary quinone forms two hydrogen bonds with its environment, one of which was shown to be highly sensitive to the Q_A state. In the case of the reduced primary quinone two stable hydrogen bond proton positions were shown to exist on $[Q_A-His^{M219}]$ hydrogen bond line, while there is only one stable proton position in the case of the oxidized primary quinone. Taking into account this fact and also the ability of proton to transfer between potential energy wells along a hydrogen bond, theoretical study of temperature dependence of hydrogen bond polarization was carried out. Current theory was successfully applied to interpret dark P^+/Q_A^- recombination rate temperature dependence.

© 2007 Elsevier B.V. All rights reserved.

Keywords: Photosynthetic reaction center; Electron transfer; Hydrogen bond; Proton tunneling; Dipole relaxation

1. Introduction

Membrane photosynthetic reaction centers (RCs) are unique objects to study electron transport mechanisms. Hydrogen bonds as essential structural components in RCs can be involved in electron transfer by participating in relaxation processes.

We have shown experimentally the existence of the effect of hydrogen bond state on energy migration processes, charge separation and stabilization in purple bacteria RCs. We observed considerable inhibition of these processes as a result of hydrogen bonds treatment by cryogenic solvents, and also after isotope replacement of H_2O by D_2O [1–3]. The technique of site directed mutations allows one to study the influence of a particular hydrogen bond within RCs on primary processes of light energy transformation. In particular, in mutant RCs, different numbers of hydrogen bonds located between bacteriochlorophyll dimer

(P) and its neighbors are responsible for changing the initial charge separation times from 3.5 ps (in the case of a single hydrogen bond) to 50 ps (4 hydrogen bonds) [4–7]. This is accompanied by a decrease in the dark charge recombination rate $P^+Q_A^- \rightarrow PQ_A$ [6].

Possible mechanism of hydrogen bond influence on charge separation rates in RCs can be due to their high sensitivity to electronic density rearrangements in a molecular system, manifested as alterations of potential energy surface of a hydrogen bond. For example, in [8] it was shown, that in photosynthetic RCs a proton located on a hydrogen bond between a secondary quinone (Q_B) and histidine residue can be found either near Q_B or in the middle of the hydrogen bond length between Q_B and histidine, depending on the electronic state of Q_B .

In the present work we investigated a molecular system, consisting of a primary quinone Q_A and its environment (Fig. 1). The system is referred below as a primary quinone model. The model was used to calculate $[Q_A-His^{M219}]$ hydrogen bond potential energy curves in case of an oxidized as well as reduced primary quinone.

* Corresponding author. Fax: +74959391115.

E-mail address: krpam@mail.ru (P.M. Krasilnikov).

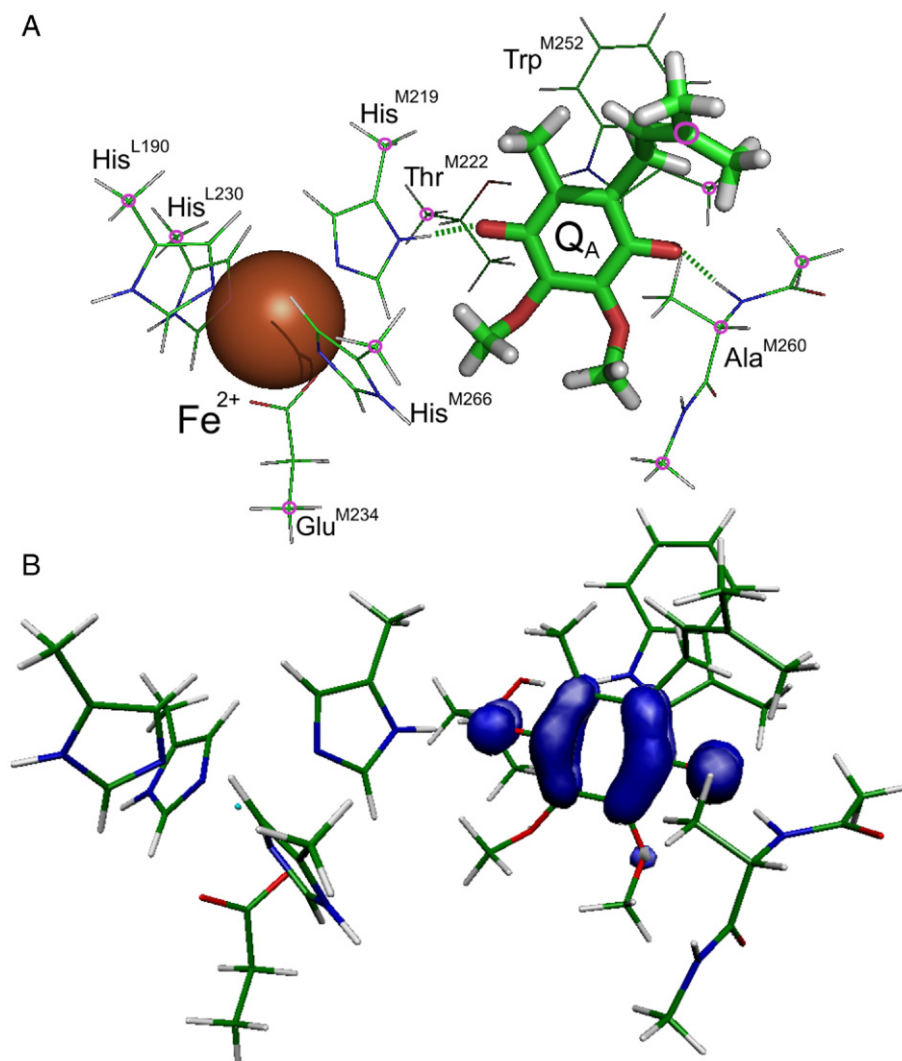


Fig. 1. The primary quinone model used for quantum chemical calculations. (A) The model includes the primary quinone Q_A molecule with the shortened tail, non-heme iron ion Fe^{2+} and neighboring amino-acid residue side-chains. Hydrogen bonds formed by primary quinone are shown by dashed lines. Heavy atoms with fixed positions are marked by circles. (B) The highest occupied molecular orbital in the case of the reduced primary quinone, i.e. an excessive electron localization area.

Results of calculations were used to analyze the experimental temperature dependence of P^+/Q_A^- charge recombination rate in *Rhodobacter sphaeroides* RCs in the temperature range from 140 up to 320 K.

2. Materials and methods

2.1. Quantum chemical calculations details

Atomic coordinates for the primary quinone model were obtained from RCSB Protein Data Bank (PDB ID: 1AIJ) [9]. The geometry of the model was further optimized in both oxidized and reduced states, fixing positions of several heavy atoms in order to retain the structure of Q_A site (see Fig. 1A). At Fig. 1B the highest occupied molecular orbital of the reduced primary quinone model (i.e. an area of localization of an excessive electron) is presented. After geometry optimization the potential energy curves of the $[Q_A-His^{M219}]$ hydrogen bond in both states were calculated (see Fig. 2). Geometry optimization as well as potential energy surface scanning were done using restricted open shell density functional

theory approach (B3LYP5 hybrid functional and 6-31G* basis set were used) [11–13]. All calculations were performed with PC GAMESS program [10].

2.2. P^+/Q_A^- recombination reaction investigation

Wild strain of purple photosynthetic bacteria *Rhodobacter sphaeroides*, 2R courtesy of the Department of Microbiology of M.V. Lomonosov Moscow State University was used in the experiments. RCs of *Rb. sphaeroides* were isolated from chromatophores by solubilization with 0.5% lauryldimethylamineoxide (LDAO) in 10 mM sodium phosphate buffer (pH 7.0) at 4 °C for 30 min. The isolation procedure is described in detail in [14]. Isolated RCs of *Rb. sphaeroides* were suspended in 10 mM sodium phosphate buffer (pH 7.0) containing 0.05% LDAO.

In order to suppress $Q_A \rightarrow Q_B$ electron transfer and to assess the temperature dependence of P^+/Q_A^- recombination rate, orthophenantroline was administrated into isolated RCs emulsion (10^{-2} mM). Samples, containing 70% vol. glycerin, were activated with single short light flashes (xeon lamp: 9 mJ; spectral band: 400–600 nm; impulse width: 10 μ s). P^+ reduction kinetic was analyzed by measuring the absorbance changes at

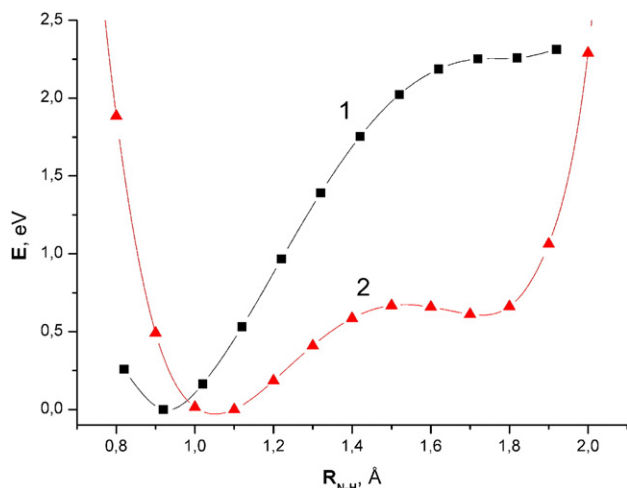


Fig. 2. Potential energy curves obtained for the primary quinone model by moving proton along $[Q_A\text{-His}^{M219}]$ hydrogen bond line. Potential energy of the model is plotted as a function of the distance between a hydrogen atom and a corresponding nitrogen atom of His^{M219} in a hydrogen bond. Potential energy minima are used as a reference point. Curve 1—potential energy curve obtained for the oxidized quinone. Curve 2—potential energy curve obtained for the reduced quinone.

870 nm with the aid of a computerized home-made one-beam differential spectrophotometer.

3. Results

3.1. Quantum chemical calculations results

Geometry optimization of the primary quinone model in both oxidized and reduced states resulted in quite similar structures. However a considerable difference was found between $[Q_A\text{-His}^{M219}]$ hydrogen bond potential energy curves obtained for the oxidized and reduced primary quinone. Corresponding curves are presented in Fig. 2. As one can see in the case of the oxidized primary quinone there is only one stable position of proton on the hydrogen bond's line and proton localizes near the corresponding nitrogen atom, farther from the corresponding quinone's oxygen atom (Fig. 1B, curve 1). The primary quinone one-electron reduction alters potential energy surface of the model. In the case of the reduced primary quinone second minimum appears on $[Q_A\text{-His}^{M219}]$ hydrogen bond potential energy curve (Fig. 1B, curve 2). So, the primary quinone reduction causes the appearance of a second stable proton position near corresponding oxygen atom of the quinone. We used this qualitative result for the interpretation of P^+/Q_A^- recombination rate temperature dependence.

3.2. Temperature dependence of P^+/Q_A^- recombination rate in *Rb. sphaeroides* RCs

Experimental investigation of P^+/Q_A^- charge recombination rate



in purple bacteria *Rhodobacter sphaeroides* RCs showed the non-monotonous temperature dependence of its characteristic time values (τ) (Fig. 3A). The initial temperature rise, is coupled to the τ rise from ~ 30 ms (at $T=77$ K) up to ~ 100 ms (at $T=270$ K). After that, in the 270–300 K temperature interval it does not change significantly. However the subsequent heating (above 300 K) causes the τ decrease (75 ms, $T=315$ K). The effect of heating up to 320 K is completely reversible—after cooling the sample, τ values are brought to those at the onset of the heating [15].

4. Theoretical analysis

4.1. P^+/Q_A^- recombination rate temperature dependence analysis

The anomalous temperature dependence of P^+/Q_A^- recombination rate when the recombination rate value decreases as the temperature rises has attracted attention for a long time. Different approaches were suggested to explain it, including thermal linear expansion of solid bodies [16], different kinetic schemes including inter-conformational transitions with different recombination times [17,18]. Such temperature dependence can be also explained using theory of electronic-vibrational interactions [19–21]. All the theories [16–21] describe quite well the increase in characteristic time values (τ) of Reaction (1) in the temperature range of 77–300 K. However, they cannot explain the τ decrease following the subsequent heating above 300 K without taking into account the details of RCs structure and dynamics. We tried to explain this temperature dependence in our papers [15,22], using a concept of a variable shape energy barrier between the centers of electron localization. Such variations can be caused by conformational changes of light polar side chains, neighboring RC's cofactors. Theoretical analysis of this effect performed in [23,24] concerned mainly the role of hydrogen bonds. In our present work anomalous temperature dependence of Reaction (1) rate is discussed taking into account the results of quantum chemical calculations.

It is known that in Reaction (1) non-radiative electron transfer takes place over a large distance (≈ 27 Å). Free energy difference ΔG between the initial ($P^+Q_A^-$) and final (PQA) states is approximately 0.5 eV in the case of *Rb. Sphaeroides* RC, and this transition is supposed to occur between the ground states [25]. The characteristic time values of Reaction (1) is approximately 30 ms in the temperature range of 77–120 K, and 100 ms at room temperature (Fig. 3A).

Characteristic time τ of electron transfer between donor and acceptor molecules depends mainly on two factors. The first one is the probability of proton tunneling between donor and acceptor, and the second one is the energy preservation condition. The energy gap between donor and acceptor electronic levels Δ in biological systems can be up to several tenths of eV. At the same time the energy preservation condition requires the energetic balance to be true for every act of tunneling. Thereby, non-radiative electron transfer in biological systems can occur only with the assistance of the

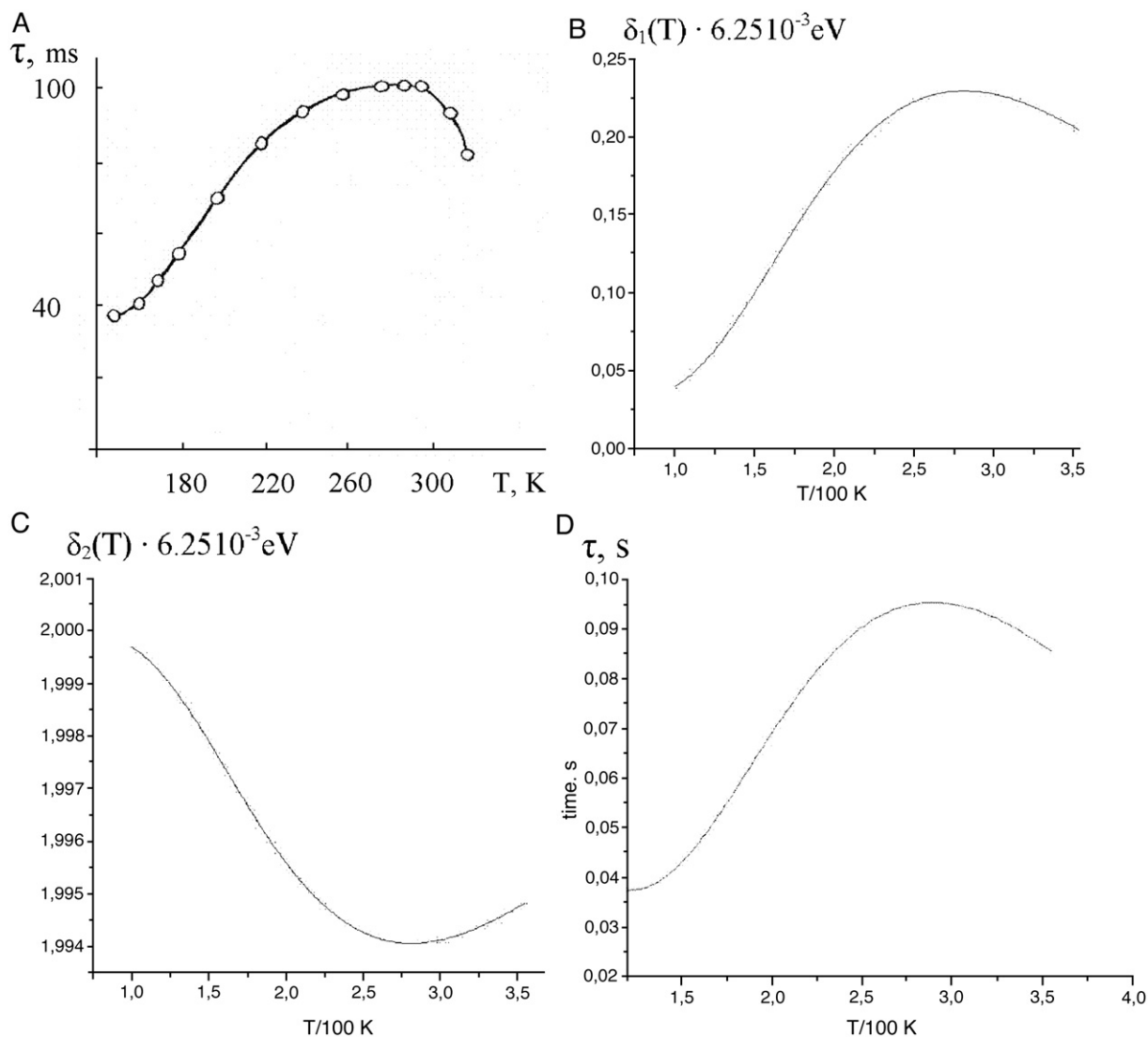


Fig. 3. Dark reduction of a photooxidized bacteriochlorophyll dimer by a primary quinone in *Rb. sphaeroides* RC. Temperature dependence characteristic time τ and δ_1 and δ_2 energy values, which determine energy gap between dimer and quinone vibrational sublevels, are presented. (A) Experimental τ temperature dependence. (B) Theoretical δ_1 temperature dependence. (C) Theoretical δ_2 temperature dependence. (D) Theoretical τ temperature dependence, obtained by taking into account interactions between an excessive electron and hydrogen bonds formed by quinone with its surrounding. Theoretical curve is in a qualitative agreement with the experimental one.

surrounding medium, as an energy reservoir. In this case electron transfer should be accompanied by different relaxation processes, such as dielectric relaxation of the media, atomic groups and chemical bonds polarization (for example—hydrogen bonds), electron–vibrational interactions (in this case proton motions in the hydrogen bond can also play a role of the accepting mode), microconformational and subsequent conformational rearrangements. All these factors are interconnected and act together, so that separate contribution of each of them to the electron transfer is unknown. Thus the detailed examination of their role is necessary, especially in the case of long range non-radiative electron transfer. Here we are going to examine two of these factors: hydrogen bonds polarization, caused by an excessive electron electrostatic field and electron–phonon interactions. Electron–phonon interaction is a kind of electron–vibrational interactions. In the case of

electron–phonon interactions the role of vibrational mode is played by low-frequency normal modes of media, called acoustic modes or phonons. Phonons are appropriate for the description of thermal equilibrium between a multiparticle system and a thermostat, as well as the heat exchange between the chosen subsystem and a thermostat. Phonon energy is distributed according Bose–Einstein statistics [26]. In the case of the uphill electron transfer one says that phonons are absorbed, i.e. energy is donated to a system by a thermostat. And vice versa, in the case of the downhill electron transfer phonons are emitted, i.e. the excessive energy is taken from a system by a thermostat.

In a recombination Reaction (1) an electron tunnels from the ground vibrational sublevel of Q_A^- to the excited vibrational sublevel of P^+ and then moves to its ground vibrational sublevel. Let us designate the energy difference between ground

vibrational sublevels of Q_A^- and P^+ as Δ . The Δ value may differ from the free energy difference ΔG , which is the total energy effect of the electron transfer. It is determined by the ability of the free energy to be partially stored and not lost in some dissipative processes. Free energy can be stored in the form of strained conformations, electrostatic interactions or excitation energy. After electron tunneling, this energy is returned to the system. Thus the energy gap Δ between electronic levels of donor and acceptor molecules is less than ΔG , by the amount of the stored energy (W), i.e. $\Delta = \Delta G - W$. In electron tunneling, the W energy is spent to excite vibrations within molecules. The less is W the more effective is electron transfer between a donor and acceptor. Let us point out, that it is total free energy change $\Delta G = \Delta + W$ that can be assessed experimentally because the W energy, which is determined by electrostatic field work, is stored within a system.

Let us discuss the physical meaning of Δ in details. Energy levels diagram of the primary quinone anion and the bacteriochlorophyll dimer cation is presented at Fig. 4A. Bold lines correspond to the ground vibrational sublevels of quinone and dimer electronic terms, and thin lines correspond excited sublevels. Obviously, the main vibrational sublevel of a quinone most likely does not overlap with N -th vibrational sublevel of a dimer. The difference between these levels is designated below as δ . Also, let us designate the energy difference between the dimer ground level and N -th vibrational sublevel as Δ_0 . Hence, one can write:

$$\Delta = \Delta_0 \pm \delta. \quad (2)$$

The value of δ is quite small, because $\delta \leq 1/2 |E_{N+1} - E_N|$, where E_N stands for energies of dimer vibrational sublevels (Fig. 4A). Electron tunneling at N -th vibrational sublevel of a dimer is only possible when the energy gap δ is compensated. This compensation is provided by electron–phonon interactions. In spite of its relatively small value ~ 0.01 eV parameter δ plays the main role in the current theory of the recombination characteristic time τ temperature dependence. Parameter δ can be represented as a sum of two energies:

$$\delta = \delta_1 + \delta_2; \quad (2')$$

where δ_1 refers to the excitation of thermal phonons, and δ_2 refers to the excitation of polarization phonons. Polarization phonons are generated by molecular structure deformation caused by electrostatic interactions between system elements, not by thermal vibrations of atoms.

Let us discuss the electron tunneling between the ground vibrational sublevel of a primary quinone Q_A^- and N -th vibrational sublevel of a dimer P^+ . Let us designate the wave function of an electron localized at the donor as ψ_Q , and the wave function of an electron localized at the acceptor as ψ_P . Hamiltonian of the system includes the energy of electrostatic interaction between the donor and the acceptor as well as the interaction energy between an electron and the surrounding. The electron wave function of the whole system can be represented as a linear combination of ψ_Q и ψ_P . Then electron wave functions of the ground state and the first

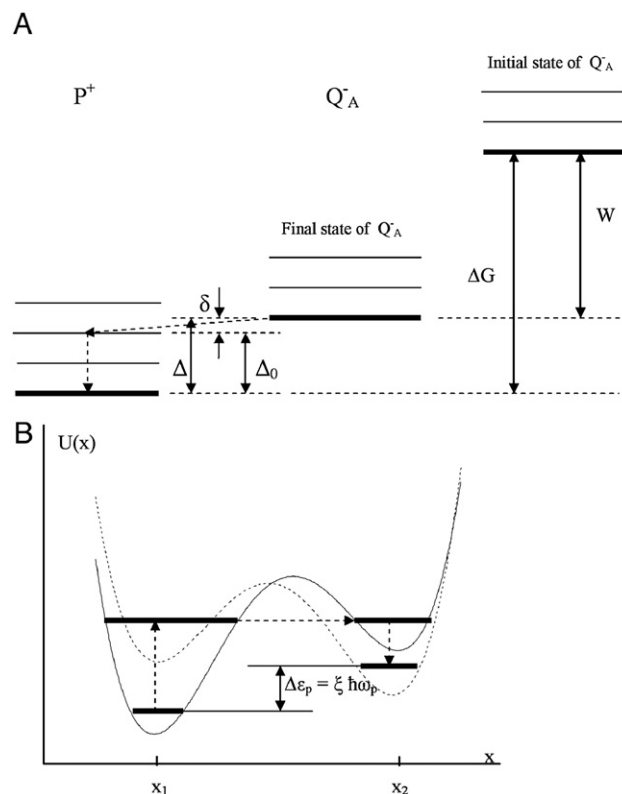


Fig. 4. Scheme of energy levels of the system in a charge separated state $P^+Q_A^-$ (A). Due to the interaction between an excessive electron and hydrogen bonds, the energy of a reduced quinone decreases, and is stored in the form of electrostatic energy. This is shown schematically in the right-hand part of the diagram. Bold lines correspond to the ground state vibrational sublevel of an electronic term. As an electron tunnels between Q_A^- and P^+ it transits from the ground vibrational sublevel of a quinone to the N -th vibrational sublevel of a dimer and then to the ground vibrational sublevel due to electron–vibrational interaction. Energy difference between excited N -th vibrational sublevel of a dimer and its ground vibrational sublevel is referred as Δ_0 . Energy detuning of quinone ground vibrational sublevel and dimer N -th vibrational sublevel is referred as δ . The scheme of hydrogen tunneling along a hydrogen bond with a double-well potential energy curve $U(x)$ (B). Arrows show the energy pathway of proton transfer from a potential well with the minimum position at x_1 to the potential well with minimum position at x_2 . The difference between proton energies when it localizes in different potential wells is referred as $\Delta \epsilon_p$. Bold arrows show dipole moments of a hydrogen bond depending on the proton position on a hydrogen bond line: μ_1 and μ_2 . Hydrogen bond potential energy profile $U(x)$ is marked by solid line in the case of proton localization in the left well. The same profile for the case of proton localization in the right well is marked by dashed line. The profiles are different due to the system relaxation after proton transfer between potential energy wells.

excited state can be obtained by performing a standard variation procedure:

$$\Psi_1 = \psi_Q + (I/\delta)\psi_P, \Psi_2 = \psi_P - (I/\delta)\psi_Q,$$

where I stands for the energy overlap integral, and δ —for the energy gap between levels, which is compensated by electron–phonon interaction. Transition between Ψ_1 and Ψ_2 states corresponds to the electron transfer between a donor and acceptor respectively. The difference between energies of these states determines the energy of either emitted or absorbed phonon. Taking into account the distance between

a donor and acceptor in the case of Reaction (1), one can approximate ψ_Q and ψ_P by wave functions of a hydrogen atom. Such approximation seems to be reasonable, since an electron can be localized either at the donor or at acceptor. Localized electronic states take place in the case of spatially finite potential energy well, whose energy is larger than electron energy. The width of this well determines spatial area of the electron localization, and can be described by the so-called localization length a . The wave function ψ , which describes the electron state within this well is determined by the shape of the potential energy surface and can be a complex function of spatial coordinates. However, outside the area of the electron localization the wave function ψ always decay, and in many cases it decays exponentially, i.e. $\psi=A(r) \exp(-r/a)$ (in the case of harmonic potential $\psi \sim \exp(-r^2/a^2)$), where $A(r)$ is a power function of coordinates). When $r \gg a$, $A(r)$ can be neglected, and an electron wave function can be approximated by a hydrogen-like electronic wave function $\psi \approx (\pi a^3)^{1/2} \exp(-r/a)$, where a stands for electron's effective localization length. The more the value of (r/a) ratio is the more realistic is such approximation. According to quantum chemical calculations, in the case of RC electron effective localization length at a quinone is approximately 1 Å (see Fig. 1). The mean distance between electron localization centers is approximately $R \approx 28$ Å. Hence $R/a \approx 28 \gg 1$ and the usage of the hydrogen-like electronic wave function does not lead to considerable errors. However it facilitates analytical evaluations of overlap integrals when calculating matrix elements. The expression for the characteristic time of electron tunneling between donor and acceptor can be obtained, using matrix element of electron–phonon interaction:

$$\tau = \frac{\pi \rho \cdot s^5 \hbar^4}{E_1^2} \left(\frac{a^2 \varepsilon}{e^2} \right)^2 \frac{1}{R^2} \left(1 + \left(\frac{\delta \cdot a}{2 \hbar s} \right)^2 \right)^4 \exp\left(\frac{2R}{a}\right) \cdot \frac{1}{\delta} \cdot q_{ph} \quad (3)$$

where ρ —density of the medium, ε —dielectric permeability \hbar ,—Plank constant, e —electron charge, a —electron localization radius, R —distance between donor and acceptor, E_1 —deformative potential constant, s —acoustic speed, q_{ph} —probability of phonon emission or absorption. As it was noted above, $\delta = \delta_1 + \delta_2$, where δ_1 refers to the excitation of thermal phonons and δ_2 —excitation of polarization phonons. Hence, q_{ph} is a product of phonon excitation probabilities $q_{ph} = q_{ph1} q_{ph2}$. The probability of thermal phonon emission q_{ph1} can be written as follows:

$$q_{ph1} = 1 - \exp(-\delta_1/kT), \quad (4)$$

where kT stands for thermal energy, k —Boltzman constant, T —absolute temperature. The probability of polarization phonon excitation is equal to $q_{ph2} = 1$. So, the temperature dependence of characteristic time τ is determined by the temperature dependence of δ and q_{ph} parameters.

Characteristic time τ , in Eq. (3), depends on the probability of electron tunneling, with the account of electron–phonon

interactions. After electron comes to N -th vibrational sublevel of a dimer, it transits further to the ground vibrational sublevel of the dimer, loosing the energy Δ_0 . This transition is accompanied by the excitation of $N = \Delta_0/\hbar\Omega$ oscillatory quanta. As shown below, N is most likely to be less than or equal to 2, though the exact value of N does not affect the results of our analysis. Indeed, an electron comes to a dimer after it has tunneled between donor and acceptor. This transition is practically irreversible. First, an electron has already lost part of the energy, which is equal to the energy of t , the emitted phonon. Second, due to electron–vibrational interactions, an electron transits to the ground vibrational sublevel of the dimer electronic term for 10^{-12} – 10^{-11} s giving to a thermostat the energy of about several tenths of eV. Hence, after an electron appears at the dimer, it transits to the ground vibrational sublevel of the dimer electronic term much faster than the Reaction (1) occurs. Hence the Reaction (1) becomes practically irreversible. Because we are interested in the characteristic time of the Reaction (1), we assume the electron transition is complete after an electron reaches any vibrational sublevel of the dimer. Also we are not interested in details of the electron–vibrational relaxation. The point is that the time of this relaxation is much shorter than the period of quantum oscillations within quinone–dimer system, which makes the Reaction (1) irreversible.

The subsequent intramolecular vibrational relaxation proceeds at approximately 10^{-12} – 10^{-11} s. Taking into account that the characteristic time of Reaction (1) is 30–100 ms, the probability of this transition, which is determined by Frank–Condon factor, can be equal to 1. According to the calculations, presented below, the value of δ as well as its variation are quite small ($\delta \ll \Delta$). Hence, $\Delta_0 = \text{const}$, i.e. an electron always comes to the same N -th vibrational sublevel of a dimer. Hence the details of the electron transition in the dimer between N -th and ground state vibrational sublevels are not significant for our further analysis.

Now let us discuss Eq. (3). Taking into account Eq. (4) one can easily find out that while temperature decreases $T \rightarrow 0$, the probability $q_{ph1} \rightarrow 1$, and the recombination time τ varies only slightly, if $\delta = \text{const}$. Let us calculate the value of τ when $T \rightarrow 0$. Parameter values are accepted as follows: $\rho = 0.9 \text{ g/cm}^3$, $\varepsilon = 3$, $a = 1 \text{ Å}$, $R = 27 \text{ Å}$, $E_1 = 2 \text{ eV}$, $s = 1.5 \times 10^5 \text{ cm/s}$, $\delta_0 \approx 0.0125 \text{ eV}$, $q_{ph} = 1$. Using these parameters values one can get the value of $\tau_0 = 30 \text{ ms}$, which is in good agreement with experimental data. However taking into account the strong τ dependence on other parameters (especially R), this estimation is in agreement with experimental data only by the order of magnitude. Now let us transform Eq. (3), by introducing a new constant $\delta_0 = 0.0125 \text{ eV}$:

$$\tau = \tau_0 F(T), \quad (3')$$

$$F(T) = \delta_0/\delta(T) \cdot (1 - \exp\{-\delta_1(T)/kT\})$$

Under the assumption $\delta(T) = \text{const}$, a temperature decrease causes the exponential decrease in recombination time τ values. This result contradicts experimental temperature

dependence (Fig. 3A). In order to solve this problem and to study the temperature dependence of $\delta(T)$ parameter, one should obtain $F(T)$ in an explicit form.

Since the process under consideration is accompanied by the emission of phonons, one should choose the plus sign in Expression Eq. (2). Now let us examine the energy gap δ_1 , taking into account that energy δ_2 is included in W . An expression for δ_1 is as follows:

$$\delta = \Delta G - \Delta_0 - W. \quad (5)$$

Hence, the temperature dependence of δ_1 is determined by the temperature dependence of the stored energy $W(T)$. In the case of Reaction (1), free energy change ΔG equals approximately to 0.5 eV. Let us examine the situation, when it is partially stored in electrostatic interactions between an excessive electron, localized at the primary quinone, and neighboring hydrogen bonds: $W = -(\mu_1 \cdot E_1) - (\mu_2 \cdot E_2)$, where μ_1, μ_2 stand for dipole moments of hydrogen bonds, E_1, E_2 are field strength vectors, produced by an excessive electron at points of dipole localization: $E_j = e/\epsilon r_j^2$, e —an elementary charge, ϵ —dielectric permeability of the medium, $r_j = \{r_1, r_2\}$ —distances between an electron and centers of the first and second hydrogen bond dipoles. These distances are measured from Q_A center because an excessive electron localizes at Q_A (Fig. 1). Quantum chemical calculations showed that $r_1 \approx r_2 \approx 4 \text{ \AA}$, partial charges of protons equals $0.4e$, and partial charges of nitrogen and oxygen atoms to approximately $0.6e$. Let us suppose dielectric permeability ϵ to be equal to 3. The angle θ_0 between μ , directed along a hydrogen bond, and electric field strength vector equals approximately 30° (Fig. 4). In the case of proton localization near the corresponding nitrogen atoms $W_{00} \approx 0.21 \text{ eV}$. Proton shifting toward Q_A oxygen atoms causes the twofold increase in W value: $W_{11} \approx 0.41 \text{ eV}$. Let us point out that this energy is returned to the system after an electron has come to a dimer. These evaluations show that the difference between energetic levels of donor and acceptor may be quite small $\Delta \approx \Delta_0 = \Delta G - W_{11} \approx 0.09 \text{ eV}$, or even smaller, if interactions between an excessive electron and some distant hydrogen bonds and water molecules are taken into account. So, due to the electrostatic interactions between an excessive electron and its surrounding, the energy gap between donor and acceptor levels decreases (Fig. 4A).

Now let us calculate a temperature dependence of $\delta_1(T)$ and establish an interval of δ_1 variations. In order to do it, one should analyze the kinetics of proton transfer along a hydrogen bond between potential energy wells. In Fig. 4B a model potential energy surface $U(x)$ of a hydrogen bond is presented, where $\Delta\epsilon_p = |\epsilon_2 - \epsilon_1|$ stands for the difference between proton energies within the first and second wells. Proton tunneling between wells can be represented as involving direct and backward reactions, with the rate constants K_1 and K_2 respectively. Using this approach, one can get well known expressions for the populations of both wells: $n_1 = K_2/(K_1 + K_2)$, $n_2 = K_1/(K_1 + K_2)$. Taking into account the energy difference $\Delta\epsilon_p$, the reaction rate constant K_1 can be represented as $K_1 = K_2 \exp(-\Delta\epsilon_p/kT)$.

Consider another important factor. The efficacy of proton tunneling along a hydrogen bond strongly depends on the bending of the latter. This deformation is determined by the angle β between a hydrogen bond line and a line connecting a proton with one of the electronegative atoms. When β becomes equal to $\sim 30^\circ$ a hydrogen bond breaks [27]. Hence, proton tunneling efficacy varies from zero in the case when $\beta > 30^\circ$ up to the highest possible value when $\beta = 0$.

Now we consider qualitatively the effect of small angular deformations of a hydrogen bond on the probability of proton tunneling. A proton atom can librate, causing hydrogen bond deformation. According to Pople [28], these librations can be described, using classical approach: $\beta(t, T) = \sqrt{kT\gamma} \sin \omega_0 t$, where γ stands for bending rigidity, $\omega_0 \sqrt{\gamma l}$ —frequency of librations, l —proton moment of inertia. The amplitude of oscillations can be determined taking into account that under thermal equilibrium equal thermal energy portions of $1/2 kT$ falls on each degree of freedom. Mean square deviation of the libration angle β^2 equals $kT/2\gamma$.

Using harmonic approach, one can find how the energy integral, determined by the proton wave functions overlap, depends on β . The integral determines the probability of the proton tunneling between potential energy wells: $p = p_0 \exp(-A \beta^2)$, where p_0 stands for the probability of proton tunneling when $\beta = 0$, $A = m\omega_p R_p l / 2\hbar$, m —proton mass, ω_p —frequency of its oscillations along the bond, R_p —the distance between electronegative atoms, l —the length of a covalent bond between proton and one of the electronegative atoms. Taking into account this effect, one can obtain the expression for the K_1 : $K_1 = K_2 \exp\{-f(T)\}$, where $f(T)$ is as follows:

$$f(T) = \frac{\Delta\epsilon_p}{kT} + \frac{AkT}{2\gamma}. \quad (6)$$

As we shall see below, function $f(T)$ depends non-monotonously on the temperature. It plays a key role in our consideration.

Let us find out an expression for the energy W of interactions between an electron and dipole moments of hydrogen bonds, taking into account the corresponding populations n_1 and n_2 of potential wells:

$$W(T) = W_{11}n_1 + W_{00}n_2, \quad (7)$$

$$n_1 = (1 + \exp\{-f(T)\})^{-1}, \quad n_2 = n_1 \exp\{-f(T)\}.$$

As one can see, W also depends on temperature non-monotonously. Indeed, the extremum (minimum) of this function is determined by the condition $df/dT = 0$. This extremum can be found by differentiating Expression Eq. (7) and solving the obtained equation for the temperature:

$$T_m = \frac{1}{k} \sqrt{\frac{2\Delta\epsilon_p \gamma}{A}}. \text{ Let us represent energy } \Delta\epsilon_p \text{ as } \xi \hbar \omega_p, \text{ where } \xi \geq 0. \text{ Parameter } \xi \text{ describes the asymmetry of a hydrogen bond}$$

potential energy curve. Using the explicit form of A , one can evaluate T_m as follows:

$$T_m = \frac{2\hbar}{k\sqrt{m}} \sqrt{\frac{\xi\gamma}{R_p l}}$$

Let us point out that this temperature value is determined mainly by the product $\xi\gamma$. Indeed, other parameters, excluding R_p , are constant and R_p can vary within 10% limit. The value of T_m also depends on proton mass $T_m \sim m^{-1/2}$, hence there should be the isotope effect.

Now let us evaluate the T_m value using the following values of parameters: $\xi=1$, i.e. $\Delta\varepsilon_c = \hbar\omega_p \approx 0.0625$ eV, $\gamma=0.236$ eV/rad² [28] (this parameter can vary considerably due to the variation of the hydrogen bond energy), $R_p \approx 3$ Å, $l \approx 1$ Å. Other parameters are fundamental constants. Using these parameter values one can obtain $T_m=281$ K, which is in an excellent agreement with experimental data (Fig. 3A). However, we are interested in the coordinate of the extremum of the function $F(T)$, which may not coincide with that of $f(T)$. This problem will be discussed below.

At the temperature T_m the function $W(T_m)$ reaches its minimal value, while $\delta_1(T_m)$ parameter according to Eq. (5) reaches its maximal value. Using Eq. (5) and also taking into account $W_{11} \approx 2 W_{00}$, one can obtain the following expression for $\delta_1(T)$:

$$\delta_1(T) = \Delta g - \frac{W_{00}}{1 + \exp\{-f(T)\}}, \quad (8)$$

where $\Delta g = \Delta G - \Delta_0 - W_{00}$. In Fig. 3B $\delta_1(T)$ curve is presented. Parameter values used for the calculation are as follows: $\Delta G \approx 0.5$ eV, $W_{00} \approx 0.21$ eV, $W_{11} \approx 2 W_{00} \approx 0.42$ eV and $\Delta_0 = N \hbar\Omega \approx 0.08$ eV. Other parameter values are similar to those used in T_m calculations. This figure shows that $\delta_1(T)$ depends on the temperature non-monotonously, while $\delta_1(T)$ remains less than Δ_0 and varies from 3×10^{-4} eV up to 1.5×10^{-3} eV.

Now let us discuss the problem of polarization phonons. In order to do it one should examine an effect of the shift of the oscillator (proton) equilibrium position under the influence of an external force. Each potential energy well where a proton oscillates is represented by the harmonic potential. External force shifts the equilibrium position of the oscillator. If a proton is under the effect of the electrostatic field generated by

an electron, this shift can be expressed as $a_i = \frac{e^2}{m_p^2 \varepsilon x_i^2}$, where x_i

is the position of the potential minimum of the i -th proton. Since the distance between the minimum positions on a hydrogen bond line is approximately 0.8 Å, the value of this shift is different for different proton stable positions. This difference determines the additional effect of the proton

localization: $g_{12} \approx \frac{e^4}{m\varepsilon^2 \omega_p^2} \left(\frac{1}{x_1^4} - \frac{1}{x_2^4} \right)$. Taking into account population values of each of the potential energy wells one can obtain the energy value, which should be compared with the

energy of the polarization phonon. In the case of two hydrogen bonds it is:

$$\delta_2 = 2g_{12} \left(1 + \frac{1}{1 + \exp(-f(T))} \right). \quad (9)$$

Using the following parameters values: $x_1=3.2$ Å, $x_2=4$ Å, $\omega_p=6 \times 10^{14}$ s⁻¹, $\varepsilon=3$, an evaluation of g_{12} gives the value of 3×10^{-3} eV. In the case of two hydrogen bonds this value is doubled. After electron transfer to a dimer, δ_2 energy is returned to the system, which is equivalent to the phonon emission of the same energy with the probability of 1, $q_{ph2}=1$. The temperature dependence of $\delta_2(T)$ is presented in Fig. 3C. This figure shows that $\delta_2(T)$ non-monotonously depends on temperature, being close to the value $6 \cdot 10^{-3}$ eV.

One can get a final expression for the recombination characteristic time temperature dependence $\tau(T)$ by substituting Eqs. (9) and (8) into Eq. (2'), Eq. (8) into Eq. (4) and the final expressions into Eq. (3'). The explicit form of this dependence is not presented here because it is too cumbersome. The temperature dependence curve $\tau(T)$ is presented in Fig. 3D. This figure shows that $\tau(T)$ depends on temperature non-monotonously and it is in a qualitative agreement with the experimental curve in Fig. 3A. The position of the maximum on the theoretical curve is at 290 K. This position of the maximum is obtained using the parameter value $\xi=1.39$, while other parameters values were the same as in previous calculations.

5. Conclusion

The objective of the present study is to investigate the mechanism of hydrogen bonds influence on the electron transfer rate in the case of the recombination between a bacteriochlorophyll dimer and primary quinone $P^+Q_A^- \rightarrow PQ_A$. The interpretation of non-monotonous recombination rate temperature dependence was suggested. According to this interpretation, primary quinone reduction alters its potential energy surface, specifically it brings about the appearance of the second potential well on the hydrogen bonds potential energy curves. This allows a proton to be transferred between the wells, i.e. it may be localized farther from or closer to the excessive electron localization site. Taking into account the population values of each of the wells, electrostatic energy of interaction between proton and the excessive electron can be estimated. This energy, being a portion of the free energy of the system, is stored and returned back to the system, after an electron is transferred back to a dimer. The probability of proton tunneling between potential energy wells determines the population of each of the wells, and depends on temperature non-monotonously. Hence, a portion of the free energy, stored as electrostatic energy of interactions between protons and an excessive electron also depends on temperature non-monotonously. This determines non-monotonous temperature dependence of P^+/Q_A^- recombination rate, since the principle of energy balance of the whole system should be valid, which is provided by electron-phonon interactions during electron tunneling. Because of the non-monotonous temperature dependence of phonon energy,

emitted while electron is transferred from quinone to a dimer, the probability of electron tunneling depends on temperature non-monotonously as well. A critical feature of the model, essential for the explanation of non-monotonous recombination rate temperature dependence is the shape of hydrogen bond potential energy curve with two minima.

We suggest that interactions between an excessive electron and hydrogen bonds play a regulatory role in electron transfer, which may be also true in other biological processes.

Acknowledgements

This study was supported by the Russian Foundation for Basic Research (Projects nos. 05-04-48912, 05-04-48606 and N.Sh. 9144.2006.4).

References

- [1] V.Z. Paschenko, B.N. Korvatovskii, S.L. Logunov, A.A. Kononenko, P.P. Knox, N.I. Zakharova, N.P. Grishanova, A.B. Rubin, Modification of protein hydrogen bonds influences the efficiency of picosecond electron transfer in bacterial photosynthetic reaction centers, *FEBS Lett.* 214 (1987) 28–34.
- [2] P.P. Knox, V.Z. I.Yu. Churbanova, On the relationship between structural and dynamic properties in purple bacteria reaction centers and stabilization of photomobilized electron on quinone acceptors, in: G. Garab (Ed.), *Photosynthesis: mechanisms and effects*, vol. 2, Kluwer Acad. Publ., Netherlands, 1998, pp. 821–824.
- [3] V.Z. Paschenko, V.V. Gorokhov, N.P. Grishanova, E.A. Goryacheva, B.N. Korvatovskiy, P.P. Knox, N.I. Zakharova, A.B. Rubin, The influence of structural-dynamic organization of RC from purple bacterium on picosecond stages of photoinduced reactions, *Biochim. Biophys. Acta* 1364 (1998) 361–372.
- [4] J.C. Williams, R.G. Alden, M.A. Murchison, J.M. Peloquin, Effects of mutations near the bacteriochlorophylls in reaction centers from *Rhodobacter sphaeroides*, *Biochemistry* 31 (1992) 11029–11037.
- [5] X. Lin, M.A. Murchison, V. Nagarajan, W.W. Parson, J.P. Allen, J.C. Williams, Specific alteration of the oxidation potential of the electron donor in reaction centers from *Rhodobacter sphaeroides*, *Proc. Nat. Acad. Sci. U. S. A.* 91 (1994) 10265–10269.
- [6] H.A. Murchison, R.G. Alden, J.P. Allen, J.M. Peloquin, A.K. Taguchi, N.W. Woodbury, J.C. Williams, Mutations designed to modify the environment of the primary electron donor of the reaction center from *Rhodobacter sphaeroides*: phenylalanine to leucine at L167 and histidine to phenylalanine at L168, *Biochemistry* 32 (1993) 3498–3505.
- [7] L. Rinyu, E.W. Martin, E. Takanashi, P. Maroti, C.A. Wraight, Modulation of the free energy of the primary quinone acceptor (QA) in reaction centers from *Rhodobacter sphaeroides*: contributions from the protein and protein–lipid (cardiolipin) interactions, *Biochim. Biophys. Acta* 1655 (2004) 93–101.
- [8] R.V. Belousov, S.V. Poltev, A.K. Kukushkin, Proton position near Q_B and coupling of electron and proton transfer in photosynthesis, *J. Phys., Condens. Matter* 15 (2003) S1891–S1901.
- [9] H.B. Stowell, T.M. McPhillips, D.C. Rees, S.M. Soltis, E. Abresch, G. Feher, Light-induced structural changes in photosynthetic reaction center: implications for mechanism of electron–proton transfer, *Science* 276 (1997) 812–816.
- [10] A.V. Nemukhin, B.L. Grigorenko, A.A. Granovsky, Molecular modeling by using the PC GAMESS program: from diatomic molecules to enzymes, *Mosc. Univ. Chem. Bull.* 45 (2) (2004) 75.
- [11] J.J.P. Stewart, Optimization of parameters for semiempirical methods I. Method, *J. Comput. Chem.* 10 (1989) 209–220; J.J.P. Stewart, Optimization of parameters for semiempirical methods II. Applications, *J. Comput. Chem.* 10 (1989) 221–264.
- [12] J.J.P. Stewart, Optimization of parameters for semiempirical methods II. Applications, *J. Comput. Chem.* 10 (1989) 221–264.
- [13] A.D. Becke, A new mixing of Hartree–Fock and local density-functional theories, *J. Chem. Phys.* 98 (1993) 1372–1377; A.D. Becke, Density-functional thermochemistry: III. The role of exact exchange, *J. Chem. Phys.* 98 (1993) 5648–5652.
- [14] N.I. Zakharova, I.Yu. Churbanova, Methods of isolation of reaction center preparations from photosynthetic purple bacteria, *Biochemistry (Moscow)* 65 (2000) 181–193.
- [15] P.M. Krasilnikov, P.P. Knox, E.P. Lukashev, V.Z. Paschenko, I.Yu. Churbanova, K.V. Shaitan, A.B. Rubin, Reaction of charge recombination between photooxidized bacteriochlorophyll and reduced primary quinone in *Rb. sphaeroides* reaction centers is accelerated under the temperatures above 300 K, *Dokl. Biochem. Biophys.* 375 (2000) 828–830.
- [16] B.J. Hales, Temperature dependence of the rate of electron transport as a monitor of protein motion, *Biophys. J.* 16 (1976) 471–480.
- [17] V.V. Gorbach, E.P. Lukashev, P.P. Knox, A.I. Komarov, A.A. Kononenko, V.N. Verkhoturlov, E.G. Petrov, A.B. Rubin, Kinetics of bacteriochlorophyll and the primary quinone acceptor ion-radicals recombination in the photosynthetic reaction centers, *Izv. AN SSSR, ser. biol. (Russ.)* 31 (1986) 11–23.
- [18] B.H. McMahon, J.D. Muller, C.A. Wraight, G.U. Nienhaus, Electron transfer and protein dynamics in the photosynthetic reaction center, *Biophys. J.* 74 (1998) 2567–2587.
- [19] J. Jortner, Temperature dependent activation energy for electron transfer between biological molecules, *J. Chem. Phys.* 64 (1976) 4860–4867.
- [20] T. Kakitani, H. Kakitani, A possible new mechanism of temperature dependence of electron transfer in photosynthetic systems, *Biochim. Biophys. Acta* 635 (1981) 498–514.
- [21] R.A. Marcus, N. Sutin, Electron transfers in chemistry and biology, *Biochim. Biophys. Acta* 811 (1985) 265–322.
- [22] P.M. Krasilnikov, P.P. Knox, V.Z. Paschenko, G. Renger, A.B. Rubin, Relaxation processes: implication for the temperature dependence of the rate of reduction of photooxidized bacteriochlorophyll by primary quinone in *Rhodobacter sphaeroides* reaction centers, *Biophysics* 47 (2002) 445–451.
- [23] V.V. Gorokhov, N.P. Grishanova, P.P. Knox, V.Z. Paschenko, G. Renger, Possible effect of structural phase transition in reaction centers of *Rhodobacter sphaeroides* on the rate of dark reduction of photooxidized bacteriochlorophyll by reduced primary quinone, *Biophysics* 48 (2003) 427–434.
- [24] P.M. Krasilnikov, D. Bashtoviy, P.P. Knox, V.Z. Paschenko, The system of hydrogen bonds of *Rhodobacter sphaeroides* reaction centers regulates the temperature dependence of the recombination of photooxidized bacteriochlorophyll and primary quinone acceptor, *Biophysics* 49 (2004) 751–756.
- [25] J.P. Allen, J.C. Williams, M.S. Graige, M.L. Paddock, A. Labahn, G. Feher, M.Y. Okamura, Free energy dependence of the direct charge recombination from the primary and secondary quinones in reaction centers from *Rhodobacter sphaeroides*, *Photosynth. Res.* 55 (1998) 227–233.
- [26] O. Madelung, *Festkörpertheorie I, II*, Springer-Verlag, Berlin, Heidelberg, New York, 1972, p. 373.
- [27] A. Luzar, D. Chandler, Effect of environment on hydrogen bond dynamics in liquid water, *Phys. Rev. Lett.* 76 (1996) 928–931.
- [28] J.A. Pople, Molecular association in liquids: II. A theory of the structure of water, *Proc. R. Soc. A205* (1951) 163–171.